ResearchGate

See discussions, stats, and author profiles for this publication at: https://www.researchgate.net/publication/342486180

Prostate-Specific Membrane Antigen-Targeted Radiopharmaceuticals in Diagnosis and Therapy for Prostate Cancer: Current Status and Perspectives

Article *in* Cancer Biotherapy and Radiopharmaceuticals · June 2020

DOI: 10.1089/cbr.2020.3603

CITATIONS
8

READS
63

5 authors, including:

Robert Thi Ta
University of Texas MD Anderson Cancer Center
3 PUBLICATIONS **25** CITATIONS
SEE PROFILE

Kalevi Kairemo
Docrates Cancer Center
269 PUBLICATIONS **4,973** CITATIONS
SEE PROFILE

All content following this page was uploaded by Robert Thi Ta on 16 March 2023.

The user has requested enhancement of the downloaded file.

UH & EURATOM Exhibit 2042-001
Fusion v. Universität Heidelberg, et al.
IPR2023-00551

CANCER BIOTHERAPY AND RADIOPHARMACEUTICALS
Volume 36, Number 3, 2021
© Mary Ann Liebert, Inc.
DOI: 10.1089/cbr.2020.3603

Review

Prostate-Specific Membrane Antigen-Targeted Radiopharmaceuticals in Diagnosis and Therapy of Prostate Cancer: Current Status and Future Perspectives

Mai Lin,[1] Robert T. Ta,[1] Kalevi Kairemo,[2,3] Dao B. Le,[1,3] and Gregory C. Ravizzini[3]

Downloaded by University of Texas MD Anderson Cancer Center from www.liebertpub.com at 03/16/23. For personal use only.

Abstract

Prostate cancer is the most common cancer to affect men in the United States and the second most common cancer in men worldwide. Prostate-specific membrane antigen (PSMA)-based positron emission tomography (PET) imaging has become increasingly popular as a novel molecular imaging technique capable of improving the clinical management of patients with prostate cancer. To date, several ^{68}Ga and ^{18}F-labeled PSMA-targeted molecules have shown promising results in imaging patients with recurrent prostate cancer using PET/computed tomography (PET/CT). Studies of involving PSMA-targeted radiopharmaceuticals also suggest a higher sensitivity and specificity, along with an improved detection rate over conventional imaging (CT scan and methylene diphosphonate bone scintigraphy) and ^{11}C/^{18}F-choline PET/CT. In addition, PSMA-617 and PSMA I&T ligands can be labeled with α- and β-emitters (e.g., ^{225}Ac, ^{90}Y, and ^{177}Lu) and serve as a theranostic tool for patients with metastatic prostate cancer. While the clinical impact of such concept remains to be verified, the preliminary results of PSMA molecular radiotherapy are very encouraging. Herein, we highlighted the current status of development and future perspectives of PSMA-targeted radiopharmaceuticals and their clinical applications.

Keywords: imaging, PSMA, radiopharmaceuticals, targeted therapy

Introduction

Prostate cancer is the most common cancer to affect men in the United States[1] and the second most common cancer in men worldwide.[2] Diagnosis and treatment of primary prostate cancer have vastly improved with advances in surgical resection, radiotherapy, hormonal therapy, and chemotherapy. Initial diagnosis typically involves cancer detection through digital rectal examination and an elevation of serum prostate-specific antigen (PSA) levels, followed by ultrasound-guided biopsy of the prostate gland.[3] Once the diagnosis of prostate cancer is established, treatment is selected according to the anatomic extent of disease (tumor, node, metastasis stage), Gleason score/tumor grade of biopsy samples, number and extent of tumor involvement in the biopsy specimens, pretreatment serum PSA levels, and more recently genomic profiling. Imaging studies can also be used in selective patients, according to the initial risk stratification. Even though various therapeutic strategies are currently available, optimized treatment can only be achieved through the precise identification of patients with truly localized versus metastatic disease. However, conventional imaging techniques such as computed tomography (CT) and bone scintigraphy used for initial staging and restaging after cancer recurrence have limited sensitivity. More recently, several new radiotracers for positron emission tomography (PET)/CT

[1]Cyclotron Radiochemistry Facility, The University of Texas MD Anderson Cancer Center, Houston, Texas, USA.
[2]Department of Nuclear Medicine and Molecular Radiotherapy, Docrates Cancer Center, Helsinki, Finland.
[3]Department of Nuclear Medicine, The University of Texas MD Anderson Cancer Center, Houston, Texas, USA.

Address correspondence to: Mai Lin; Cyclotron Radiochemistry Facility; The University of Texas MD Anderson Cancer Center; 1881 East Road, Houston, TX 77054, USA
E-mail: **mlin2@mdanderson.org**

UH & EURATOM Exhibit 2042-002
Fusion v. Universität Heidelberg, et al.
IPR2023-00551

Downloaded by University of Texas MD Anderson Cancer Center from www.liebertpub.com at 03/16/23. For personal use only.

imaging of prostate cancer have become clinically available in the United States.[4] Nevertheless, identifying sites of active disease remains challenging when the tumor burden is low; therefore, new and more sensitive imaging techniques are warranted.

Prostate-specific membrane antigen (PSMA)-based PET imaging is emerging as an important tool for the management of prostate cancer patients. Moreover, PSMA radioligands can be modified to deliver systemic targeted radiotherapy to tumor cells and serve as a theranostic tool in the evaluation of post-therapy response. The aim of this article is to provide an overview of the recent advances in PSMA-targeted radiopharmaceuticals and their application in initial staging and restaging of prostate cancer. In addition, as some of these radiopharmaceuticals can also be used to predict response of PSMA-targeted therapy through real-time *in vivo* assessment of PSMA expression, the use of PSMA constructs as theranostic agents will also be discussed.

Antibody-Based Radiopharmaceuticals in PSMA-Targeted Imaging and Therapy

PSMA is a type II transmembrane glycoprotein that comprises (1) a 19-amino-acid internal portion, (2) a 24-amino-acid transmembrane portion, and (3) a 707-amino-acid external portion.[5,6] It was originally characterized by the murine monoclonal antibody (mAb) 7E11-C5.3.[7] Although lower level of PSMA expression can be observed in normal tissues other than prostate such as kidney, liver, small intestine, and brain,[8,9] PSMA is highly expressed in prostate cancer cells and in nonprostatic solid tumor neovasculature.[10] In fact, PSMA is reported to be overexpressed 100–1000 fold in 95% of prostate cancer cells.[11]

As 7E11 is the first anti-PSMA antibody that recognizes and binds a PSMA intracellular or cytoplasmic epitope, ^{111}In-labeled 7E11 (ProstaScint™) has been investigated clinically for imaging recurrent and metastatic prostate cancer after approval by the U.S. Food and Drug Administration in 1996 as a single photon emission computed tomography (SPECT) radiopharmaceutical.[12,13] The overall sensitivity and specific activity of ProstaScint is 60% and 70%, respectively.[14–16] However, since PSMA intracellular epitopes are only accessible during the membrane disruption process in dead, dying, or apoptotic cells, the use of ProstaScint for clinical diagnosis is limited.[17] Consequently, a humanized mAb huJ591 (J591) that targets to the extracellular domain of PSMA was developed for imaging and therapy of prostate cancer.

J591 has been studied extensively in preclinical models and demonstrated excellent tumor binding specificity in the prostate cancer xenografts.[18] According to the recent phase I/II study of ^{89}Zr ($T_{1/2}$: 78.4 h; β^+: 23%; $E_{\beta+\max}$: 0.90 MeV) labeled J591 as a PET imaging agent for metastatic prostate cancer, the overall accuracy of ^{89}Zr-J591 was 95.2% for osseous lesions and 60% for soft-tissue lesions.[19] While ^{89}Zr-J591 PET is comparable to CT and ^{18}F-FDG PET in monitoring soft-tissue lesions, ^{89}Zr-J591 imaging demonstrates superior targeting of bone lesions.

J591 is also currently the only humanized mAb used to targeted radiation therapy directly to the tumor cells.[20] Although it was initially labeled with ^{213}Bi and evaluated as a promising targeted α-particle therapeutic agent,[21] the limited availability of the ^{225}Ac/^{213}Bi generator system hampers the further application of ^{213}Bi-J591 in clinical use. As a result, J591 was labeled with ^{90}Y or ^{177}Lu for clinical evaluations. Based on the clinical trials performed in Cornell University, the maximum tolerated dose (MTD) of ^{177}Lu-J591 in a single dose is significantly higher compared with ^{90}Y-J591 (2590 vs. 647.5 MBq/m^2).[22] The MTD of ^{177}Lu-J591 can further be increased to 3330 MBq/m^2 when applying dose fractionation (two doses apart of 1665 MBq/m^2, 2 weeks apart).[22] Although myelosuppression is the dose limiting toxicity, it can be overcome through dose fractionation or in combination with other chemotherapeutic agents to stabilize the progression of prostate cancer.[23] However, because small molecules are advantageous in faster blood clearance and better tumor permeability over much larger constructs such as monoclonal antibodies, the focus of current investigative efforts is therefore switched to develop PSMA inhibitor-based radiopharmaceuticals, as they are typically small molecular agents.

Advancement of PSMA Inhibitor-Based Radiopharmaceuticals in Imaging Prostate Cancer

The enzymatic activity of PSMA is considered part of the catalytic zinc metallopeptidase family M28. Although PSMA is encoded by folate hydrolase 1 gene (*FOLH1*) that reflects its major role in folate uptake, PSMA usually acts as a glutamate carboxypeptidase II in different tissues and hydrolyzes *N*-acetylaspartylglutamate (NAAG).[24,25] Therefore, derivatives based on NAAG were developed as PSMA inhibitors and evaluated for their targeting capabilities.

Phosphorous-based compounds such as 2-phosphonomethyl pentanedioic acid and 4,4′-phosphinicobis(butane-1,3-dicarboxylic acid) were the first designed ligands with high affinity toward PSMA <1 nM.[26,27] However, due to the high polarity and relatively poor pharmacokinetic profiles of these compounds, their clinical applications are limited.[28]

Several variants of the thiol-, hydroxamate-, and sulfonamide-containing compounds were subsequently evaluated as an alternative to phosphorus-containing molecules as they demonstrated enhanced membrane permeability and oral bioavailability.[29–32] However, their clinical applications are hampered by their relatively low PSMA selectivity and metabolic stability.[28] To overcome the limitations that have occurred in the aforementioned compounds, extensive structure-activity studies were performed and yielded to a series of urea-based ligands. Many of these urea-based ligands are found to be highly specific toward PSMA, thus have been further applied for diagnostic and therapeutic purposes.

^{11}C-MCG/^{11}C-DCMC

^{11}C-MeCys-C(O)-Glu (^{11}C-MCG/^{11}C-DCMC) (Fig. 1) is the first urea-based radiotracer that targets PSMA. Although this compound was initially reported in 2002,[33] its preclinical evaluation for imaging prostate cancer was not revealed until 2005.[34] The biodistribution of ^{11}C-MCG/^{11}C-DCMC was conducted in the mice bearing with MCF-7 (breast,

UH & EURATOM Exhibit 2042-003
Fusion v. Universität Heidelberg, et al.
IPR2023-00551

Downloaded by University of Texas MD Anderson Cancer Center from www.liebertpub.com at 03/16/23. For personal use only.

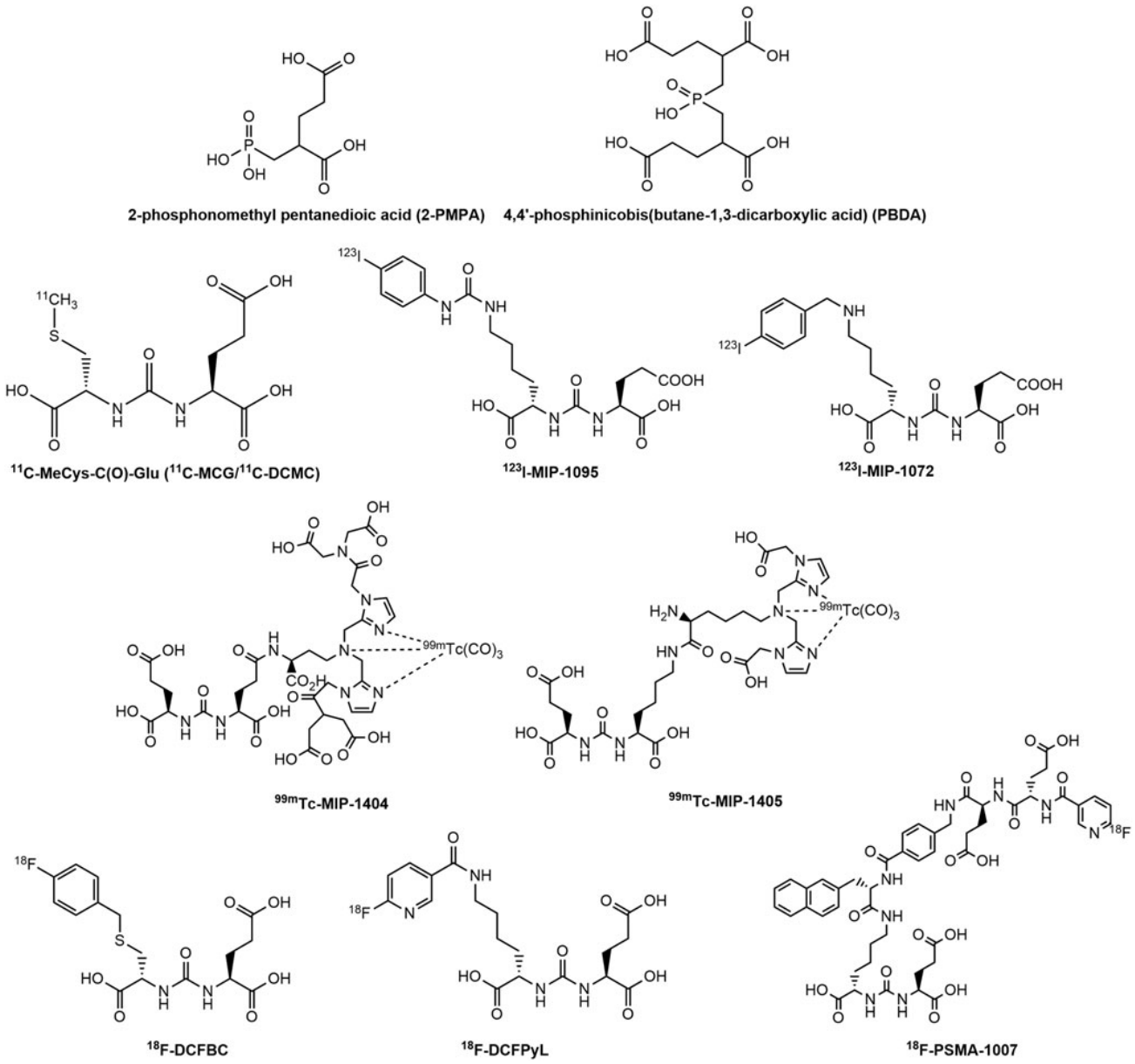

FIG. 1. Chemical structures of PSMA inhibitor-based radiopharmaceuticals. PSMA, prostate-specific membrane antigen.

PSMA-negative), PC-3 (prostate, PSMA-negative), and LNCaP (prostate, PSMA-positive) xenografts. The tracer showed high tumor-to-muscle (T/M) ratio in LNCap-derived tumors (10.78) and significantly low T/M ratios in MCF-7- and PC3 counterparts (1.28 and 2.10, respectively). The biodistribution aligned with the small animal PET imaging results and these encouraging data were further initiated an extensive research on urea-based radiopharmaceuticals in PSMA-targeted imaging and therapy.

^{123}I-MIP-1072 and ^{123}I-MIP-1095

Sodium [^{123}I]iodide is a radiotracer used for SPECT or SPECT/CT scans with a half-life of 13.2 h. Molecular Insight Pharmaceuticals, Inc. (acquired by Progenics Pharmaceuticals, Inc. in 2013) initiated a program in 2006 to develop a series of radio-conjugates for prostate cancer imaging and therapy.[35] ^{123}I-MIP-1072 and ^{123}I-MIP-1095 (Fig. 1) are the two lead compounds that showed high PSMA binding affinity. The pilot clinical studies of ^{123}I-MIP-1072 and ^{123}I-MIP-1095 demonstrated these two radiotracers as useful PSMA-targeting SPECT agents.[36] Derived from this promising result, the phase I clinical study of ^{131}I-MIP-1095 has recently been reported regarding its therapeutic efficacy in men with metastatic castration-resistant prostate cancer, in which a PSA decline of ≥50% was achieved in 70.6% of the patients (total patient number: 36) from the initial treatment. However, after the initial treatment, the group observed that ^{131}I-MIP-1095 became less effective and resulted in more frequent and intense side-effects to the patients, especially hematologic toxicities and xerostomia.[37]

UH & EURATOM Exhibit 2042-004
Fusion v. Universität Heidelberg, et al.
IPR2023-00551

^{99m}Tc-MIP-1404 and ^{99m}Tc-MIP-1405

Technetium-99m (^{99m}Tc) is the most commonly used SPECT isotope with a half-life of 6 h. Although multiple urea-based PSMA ligands labeled with ^{99m}Tc have been developed in the past decade,[38–41] only ^{99m}Tc-MIP-1404 and ^{99m}Tc-MIP-1405 (Fig. 1) were clinically evaluated.[42,43] According to the pilot SPECT scans of ^{99m}Tc-MIP-1404 and ^{99m}Tc-MIP-1405 in patients with metastatic prostate cancer, Vallabhajosula et al. observed that both tracers are able to identify most metastatic lesions in bone and soft tissues (Fig. 2).[43] However, because ^{99m}Tc-MIP-1404 has relatively low accumulation in the bladder, its potential for staging and monitoring treatment response in patients with prostate cancer was further evaluated.

A recent clinical study conducted by Schmidkonz et al., which involved 93 patients with histologically confirmed prostate cancer, showed an overall positive ^{99m}Tc-MIP-1404 SPECT/CT detection rate of 97%. In addition, interobserver agreement was high for the overall scan result (97%), as well as for the detection of the primary tumor (97%), of lymph node metastases (97%), and of bone metastases (99%).[42] When applying ^{99m}Tc-MIP-1404 SPECT/CT to assess the treatment response in patients with metastatic prostate cancer through the same research group, its concordance rate to biochemical response based on the change of PSA levels was found to be 75%.[44] These encouraging results suggest a possible role of ^{99m}Tc-MIP-1404 SPECT/CT for staging and monitoring treatment in patients with prostate cancer.

^{68}Ga-PSMA-11

Gallium-68 (^{68}Ga) is a short-lived radionuclide ($T_{1/2}$: 68 min) and primarily decays through positron emission (87.94%) with a maximum energy of 1.9 MeV (mean energy: 0.89 MeV). When Obninsk first made a commercially available ^{68}Ge/^{68}Ga generator that could be eluted by dilute hydrochloric acid to provide cationic ^{68}Ga in 1996,[45] it opened new possibilities of ^{68}Ga in preclinical and clinical applications. As cationic ^{68}Ga is able to form stable complexes with chelators (e.g., diethylenetriaminepentaacetic acid, 1,4,7,10-tetraazacyclododecane-1,4,7,10-tetraacetic acid [DOTA], etc.) that have already been widely used to the agents for magnetic resonance imaging (MRI) and SPECT, the amount of ^{68}Ga related research has greatly increased since 2000, especially after the first successful clinical trial of ^{68}Ga-DOTATOC in 2001.[46]

Among all PSMA inhibitor-based radiopharmaceuticals, ^{68}Ga-PSMA-11 (Fig. 1) is perhaps the most investigated PET agent for imaging prostate cancer. Afshar-Oromieh et al. initiated the evaluation of ^{68}Ga-PSMA-11as a novel PET agent for prostate cancer.[47] The researchers found that ^{68}Ga-PSMA-11 detects recurrent and metastatic prostate cancer through binding to the extracellular domain of PSMA and through internalization of the compound/agent into the cell. Since then, multiple studies have been conducted to compare ^{68}Ga-PSMA-11 with other conventional PET tracers for imaging patients with prostate cancer.

A recent prospective study conducted by Caroli et al.,[48] which involved 314 patients with recurrent prostate cancer, showed an overall positive ^{68}Ga-PSMA-11 PET/CT detection rate of 62.7%. The accuracy was increased with increasing PSA values: 42% for 0–0.2 ng/mL, 58% for 0.2–1.0 ng/mL, 75% for 1.0–2.0 ng/mL, and 94.8% for >2.0 ng/mL. In addition, the researchers found that of the 88 patients with negative fluorine ^{18}F-choline PET/CT scans, 59 (67%) were positive on ^{68}Ga-PSMA-11 PET/CT. Of these positive scans, 57% had a PSA value <2.0 ng/mL and 81% had a Gleason score of ≥7. In agreement to these findings, a positive ^{11}C-choline PET/CT detection rate was also reported with poor correlation when patients had a PSA value <2.0 ng/mL.[49]

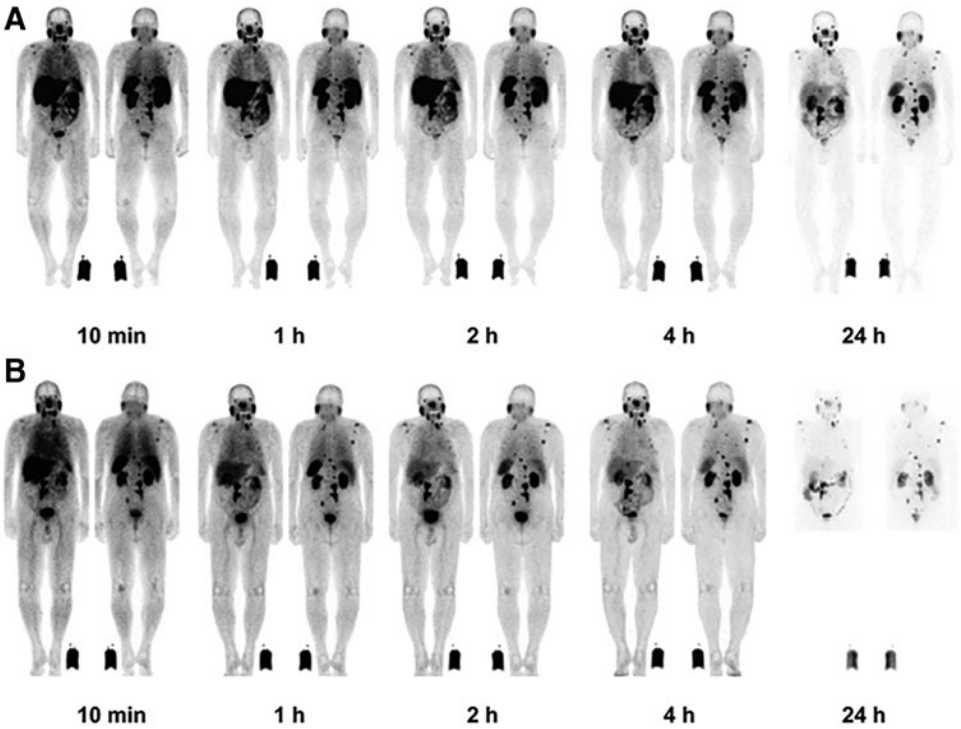

FIG. 2. Whole-body planar images of ^{99m}Tc-MIP-1404 **(A)** and ^{99m}Tc-MIP-1405 **(B)** at different times after intravenous injection showing biodistribution in patient with metastatic prostate cancer. Reprinted with permission from Journal of Nuclear Medicine, originally published by Vallabhajosula et al.[43]

Downloaded by University of Texas MD Anderson Cancer Center from www.liebertpub.com at 03/16/23. For personal use only.

UH & EURATOM Exhibit 2042-005
Fusion v. Universität Heidelberg, et al.
IPR2023-00551

Downloaded by University of Texas MD Anderson Cancer Center from www.liebertpub.com at 03/16/23. For personal use only.

With encouraging results continuously shown in prospective studies and meta-analysis,[2,48–54] several analogs based on PSMA-11 have also been evaluated as potential imaging agents for prostate cancer.[55–59] Among these molecules, PSMA-617 (Fig. 1) has received the most clinical attention. Through preclinical studies, Benesova et al. observed that the binding affinity of PSMA-617 is significantly improved toward PSMA (*Ki* for PSMA-11: 12 ± 2.8 nM, PSMA-617: 2.3 ± 2.9 nM), as well as its internalized ratio into prostate cancer cells (internalized ratio for PSMA-11: $9.47\% \pm 2.56\%$ injected activity/10^6 LNCaP cells, PSMA-617: $17.67\% \pm 4.34\%$ injected activity/10^6 LNCaP cells).[60] As DOTA is used as a chelator for PSMA-617, this tracer can be labeled with ^{68}Ga, ^{111}In, ^{177}Lu, ^{90}Y thus served as a theranostic agent; however, when comparing with ^{68}Ga-PSMA-11, although both tracers showed the highest uptake in the kidneys and salivary glands,[57,61] the pharmacokinetics of ^{68}Ga-PSMA-617 is slower in patients. Because most nuclear medicine clinical workflow is designed to conduct PET/CT scans within 1 h after injection of ^{68}Ga-labeled tracers, it remains unclear if ^{68}Ga-PSMA-617, even with its higher PSMA binding affinity and internalization nature, could detect more prostate cancer lesions than ^{68}Ga-PSMA-11. Therefore, ^{68}Ga-PSMA-11 with its putatively faster clearance provides a clear advantage over ^{68}Ga-PSMA-617.

In addition to imaging patients with recurrent prostate cancer, ^{68}Ga-PSMA-11 PET/CT can also be a valuable tool for evaluating primary prostate cancer and detecting lymph node and bone metastases. Kabasakal et al. imaged 28 prostate cancer patients with ^{68}Ga-PSMA-11 PET/CT either 5 or 60 min postinjection (p.i.) and found that images acquired on the early time point (5 min p.i.) can help better distinguish between urinary bladder and tumor lesions.[62] Perveen et al. further confirmed this observation by performing dynamic ^{68}Ga-PSMA-11 PET/CT in 15 prostate cancer patients within a time frame of 1–10 min and then compared these images to the static ones that were acquired between 45 and 60 min after injection from the same patients.[63] In their own experience, the authors observed that ^{68}Ga-PSMA-11 PET/CT occasionally reveals metastases from prostate cancer to unusual locations, such as the skin (Fig. 3). In this case, their images demonstrate a tiny 3 mm skin lesion in the perineum, which explained the patient's rising PSA levels. After the metastasis was removed, the PSA normalized. This tiny metastatic lesion was confirmed by histology and PSA-immunohistochemical staining.

^{18}F-DCFBC, ^{18}F-DCFPyL, and ^{18}F-PSMA-1007

Fluorine-18 (^{18}F) is the most widely used PET isotope. This is because ^{18}F can be produced through a medical cyclotron (9–20 MeV) with a great amount of activity and its excellent decay characteristics ($T_{1/2}$: 109.7 min, β^+ branch ratio: 97%, E_{max}: 0.633 MeV). The ^{18}F-labeled PSMA inhibitors start to receive great attention after ^{18}F-DCFBC and ^{18}F-DCFPyL (Fig. 1) were reported.

^{18}F-DCFBC is structurally similar to ^{11}C-DCMC and was initially reported in 2008.[64] In 2012, its pilot clinical PET/CT studies were performed in 5 patients with radiological evidence of prostate cancer.[65] According to the report, 32 PET-positive suspected metastatic sites were identified, with 21 concordant on both PET and conventional imaging for abnormal findings compatible with metastatic disease. Of the 11 PET-positive sites not identified on

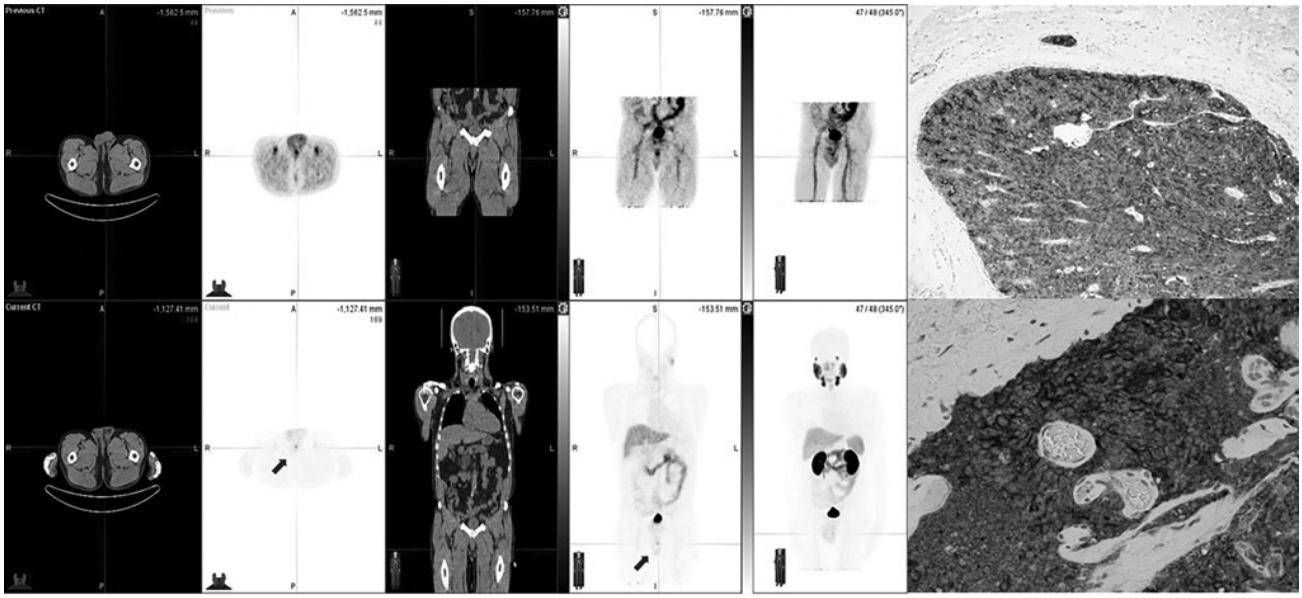

FIG. 3. ^{68}Ga-PSMA-11 imaging at 15 min (*upper row*) and at 60 min (*lower row*). This 67-year-old man had originally Gleason Score 8 prostate cancer, treated initially with transurethral resection of the prostate, androgen deprivation, and external beam radiation therapy, but developed 4 years later mediastinal lymph node metastases. The patient was then treated with docetaxel and abiraterone, but 2 years later rising PSA was detected (PSA was 3.1 ng/dL). A 3 mm perineum metastasis was identified, better depicted in the *lower row* images (*arrows*). It was surgically removed; histology (*upper right* image) revealed malignant histology and immunohistochemistry (*lower right* image) with PSA staining proved. PSA, prostate-specific antigen.

UH & EURATOM Exhibit 2042-006
Fusion v. Universität Heidelberg, et al.
IPR2023-00551

Downloaded by University of Texas MD Anderson Cancer Center from www.liebertpub.com at 03/16/23. For personal use only.

conventional imaging, most were within the bone and could be considered suggestive for the detection of early bone metastases. In a comparison of ^{18}F-DCFBC with ^{99m}Tc-methylene diphosphonate (MDP) bone scan and contrast-enhanced CT of the chest, abdomen, and pelvis in 17 patients, ^{18}F-DCFBC PET/CT has better sensitivity and was superior to detect lymph nodes, bone lesions, and visceral lesions than these imaging modalities.[66] With these encouraging clinical findings, the correlation of ^{18}F-DCFBC PET/CT with multiparametric MRI (mpMRI) and histopathology has recently been investigated.[67] However, although ^{18}F-DCFBC PET/CT has a higher positive predictive value suggesting a potential role in patients at high risk for biopsy, relatively low sensitivity (36%) of ^{18}F-DCFBC PET/CT was observed compared with mpMRI (96%) in detecting all tumor lesions at 13 patients.

Following the clinical success of ^{18}F-DCFBC, ^{18}F-DCFPyL is the next generation of ^{18}F labeled PSMA inhibitor-based radiopharmaceutical. Although the design of both tracers is based on Lys-urea-Glu pharmacophore, the ^{18}F is introduced through a fluorinated pyridine derivative that is connected to Lys to yield a more stable amide bond with the pharmacophore. Compared to ^{18}F-DCFBC, ^{18}F-DCFPyL is reported to have superior binding affinity toward PSMA (Ki for ^{18}F-DCFBC: 13.5 nM; Ki for ^{18}F-DCFPyL: 1.1 nM).[64,68] Based on the initial evaluation of ^{18}F-DCFPyL in 9 patients with prostate cancer, its biodistribution profile is superior to that observed with ^{18}F-DCFBC, exhibiting higher tumor-to-blood and tumor-to-muscle contrasts.[69] Furthermore, a secondary analysis of 8 patients in this initial clinical trial showed that a markedly increased number of lesions were visible on ^{18}F-DCFPyL PET/CT in comparison to conventional imaging with CT and MDP bone scan. When taking into account intra-patient clustering effects through use of a general estimating equation regression model, it was estimated that a proportion of 0.72 of the lesions that would be negative or equivocal with CT and MDP bone scan would be definitively positive with ^{18}F-DCFPyL PET/CT, whereas only an estimated proportion of 0.03 of the lesions that would be negative or equivocal with ^{18}F-DCFPyL PET/CT would be definitively positive on conventional imaging. These findings were in agreement with a case report comparing ^{18}F-DCFPyL PET/CT with ^{18}F-NaF PET/CT and MDP bone scans in a patient with extensive bone metastatic prostate cancer, in which several putative sites of disease were only revealed by ^{18}F-DCFPyL PET/CT (Fig. 4).[70] In recently reported clinical trial, a total of 248 consecutive patients with biochemically recurrent prostate cancer were evaluated and underwent scanning with ^{18}F-DCFPyL PET/CT. Scan positivity is correlated with the PSA values: 17/29 scans (59%) with PSA values <0.5 ng/mL; 20/29 (69%) with PSA 0.5 to <1.0 ng/mL; 35/41 (85%) with PSA 1.0 to <2.0 ng/mL; 69/73 (95%) with PSA 2.0 to <5.0 ng/mL; and 73/76 (96%) with PSA ≥5.0 ng/mL. These results appear to be comparable to those reported for ^{68}Ga-PSMA-11, with potentially increased detection efficacy compared to ^{68}Ga-PSMA-11 for patients with PSA <2.0 ng/mL.[71]

In addition to ^{18}F-DCFBC and ^{18}F-DCFPyL, ^{18}F-PSMA-1007 (Fig. 1) is another promising tracer that has recently been introduced clinically.[72] According to the meta-analysis by Treglia et al.,[73] ^{18}F-PSMA-1007 and ^{18}F-DCFPyL have similar detection rate in patients with biochemical recurrent prostate cancer. However, nonurinary excretion of ^{18}F-PSMA-1007 might be advantageous over ^{68}Ga-PSMA-11 and ^{18}F-DCFPyL in cases of local recurrence and unclear lesions in proximity to the ureter or urinary bladder (Fig. 5).[74,75]

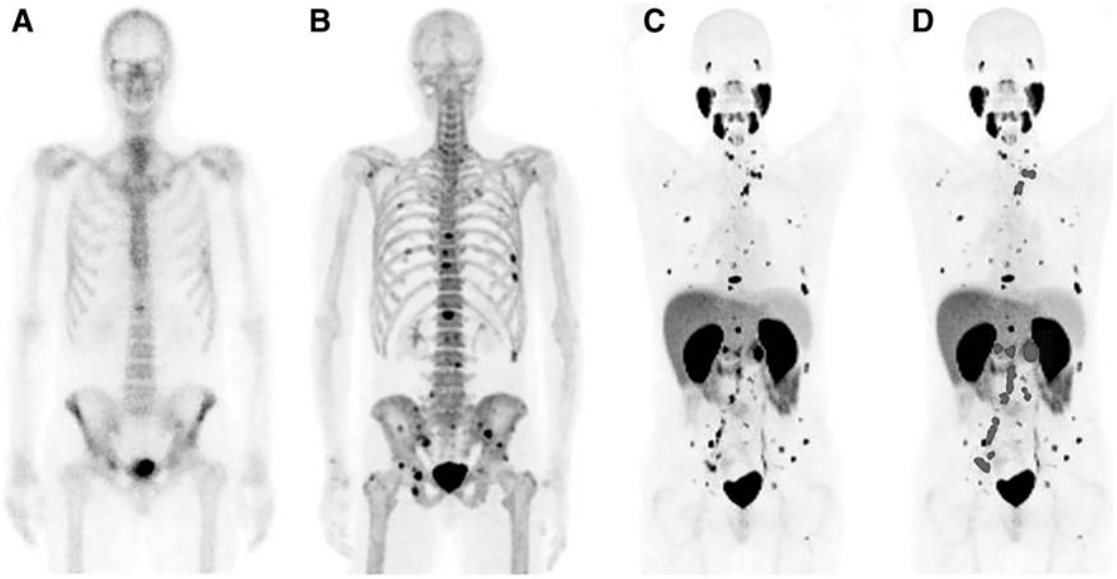

FIG. 4. **(A)** Anterior projection whole body planar ^{99m}Tc-MDP bone scan, **(B)** anterior view of the MIP from the Na^{18}F PET, **(C)** anterior view of the MIP from the ^{18}F-DCFPyL PET, and **(D)** anterior view of the MIP from the ^{18}F-DCFPyL PET with sites of abnormal radiotracer uptake within lymph nodes masked with a *red* overlay. Note the increasing number of visible lesions with Na^{18}F PET relative to ^{99m}Tc-MDP bone scan and with ^{18}F-DCFPyL PET relative to either of the other two modalities. Reprinted with permission from Clinical Genitourinary Cancer, originally published by Rowe et al.[70] PET, positron emission tomography; MDP, methylene diphosphonate.

UH & EURATOM Exhibit 2042-007
Fusion v. Universität Heidelberg, et al.
IPR2023-00551

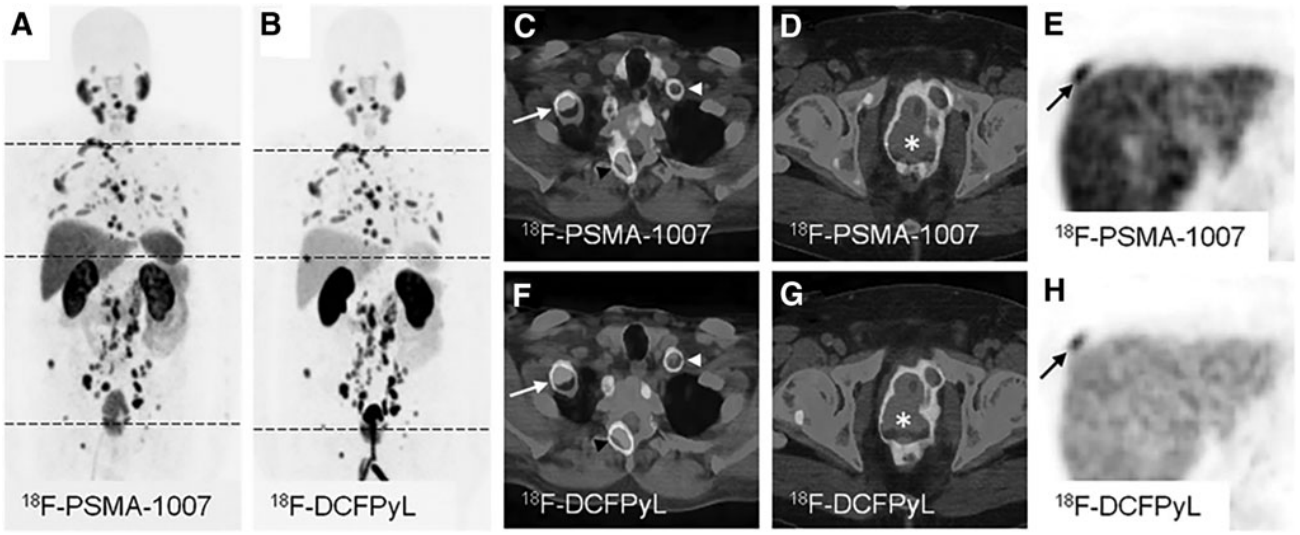

FIG. 5. Maximum-intensity projections of PET examinations using ^{18}F-PSMA-1007 **(A)** and ^{18}F-DCFPyL **(B)**, as well as exemplary PET/CT and CT cross-sections with bone and lymph node metastases **(C**, **E**, **F**, and **H)** and local tumor **(D**, **G)**. The 82-year-old patient presented with PSA serum level of 240.0 ng/mL at time of examinations. Subject was diagnosed with highly advanced metastatic prostate cancer (Gleason 9 [5 + 4]) and was treatment naive at the time of the examinations. The SUV_{max} values were 22.80 and 19.69 in the prostate [**(D**, **G)**, *asterisk*], 16.50 and 11.20 in an exemplary lymph node [**(C**, **F)**, *white arrowhead*], and 16.20 and 13.72 [**(C**, **F)**, *white arrow*] and 25.45 and 24.90 **(A**, **D)** in exemplary bone lesions for ^{18}F-DCFPyL and ^{18}F-PSMA-1007, respectively. The maximum-intensity projections **(A**, **B)** demonstrate a bone lesion that could be missed on the ^{18}F-PSMA-1007 maximum-intensity projection **(A)**. However, it is delineable on transaxial cross-sections [**(E**, **H)**, *black arrow*]. This lesion presents with SUV_{max} values of 23.72 and 17.97 for ^{18}F-DCFPyL and ^{18}F-PSMA-1007, respectively. This case highlights differences in biodistribution of tracers and similar uptake in all tumor lesions. A urinary catheter is also seen. Reprinted with permission from Journal of Nuclear Medicine, originally published by Giesel et al.[75] CT, computed tomography.

Downloaded by University of Texas MD Anderson Cancer Center from www.liebertpub.com at 03/16/23. For personal use only.

PSMA Molecular Radiotherapy

Interest in PSMA molecular radiotherapy (MRT) has been greatly increased with the recent success of the ^{177}Lu-DOTATATE (LUTATHERA®) trial showing markedly longer progression-free survival and a significantly higher response rate than high-dose octreotide of long-acting release among patients with advanced midgut neuroendocrine tumors.[76] The goal of MRT is to precisely deliver as much radiation as possible to the cancer cells but with minimal effect in the normal organs/tissues. With continuous advancement of PSMA-targeted radiotracers, theranostic agents which share the same constructs are now under investigation for the treatment of metastatic castration resistant prostate cancer.

^{177}Lu-PSMA-617 is currently most studied PSMA MRT agent, and its first retrospective multicenter cohort study comprising 145 patients from 12 centers in Germany has been published in 2017.[77] These patients received up to four MRT cycles of ^{177}Lu-PSMA-617 (range of administered activity 2–8 GBq; 5.9 GBq in average). After a single treatment, 66% of the patients experience the decrease of PSA, and a PSA decrease of more than 50% was observed in 40% of the patients. Side-effects, including mild hematotoxicity, as well as mild but transient xerostomia, were found in 10% and 8% of the patients, respectively. The promising response rates and a low toxicity nature of ^{177}Lu-PSMA-617 have also been confirmed by other recent clinical evaluations.[78–83]

In addition to ^{177}Lu-PSMA-617, the therapeutic efficacy of ^{177}Lu-PSMA I&T (Fig. 6) has received great attention in recent years as well. According to the clinical report from Kulkarni et al., although both radiopharmaceuticals share similar biodistribution profiles, the whole-body dose was moderately higher for ^{177}Lu-PSMA-617.[84] Like ^{177}Lu-PSMA-617, very little toxicity has been observed in clinical routine practice in European centers.[85] Figure 7 demonstrates the time-activity behavior using a therapeutic dose of ^{177}Lu-PSMA I&T and whole-body imaging at 0.5, 4, 24, and 168 h. The targeting signal increases throughout the study.

Although ^{177}Lu-PSMA-617 and ^{177}Lu-PSMA I&T studies have shown convincing therapeutic response in terms of both serum PSA level and radiologic findings, about 30% of patients were not responsive and dose escalation was severely limited by chronic hematological toxicity.[77,86] As a result, targeted α-therapy (TAT) that could potentially prevent radioresistance to β-emitters such as ^{177}Lu and reduce hematological toxicity has recently received great attention. The PSMA TAT was initiated by Kratochwil et al. with the administration of ^{225}Ac-PSMA-617 in 2 patients.[87] The PSA of both patients declined to undetectable levels (<0.1 ng/mL), and lesions showed a complete response on imaging. With this encouraging result, ^{225}Ac-PSMA-617 has further been investigated in 17 chemotherapy-naive patients leading to a ≥90% decline in serum PSA in 82% of patients. Importantly, 41% of these patients remained in remission 12 months after therapy.[88] While xerostomia was the primary side-effect, no severe hematologic toxicity was observed. Therefore, these preliminary results warrant further clinical evaluations.

UH & EURATOM Exhibit 2042-008
Fusion v. Universität Heidelberg, et al.
IPR2023-00551

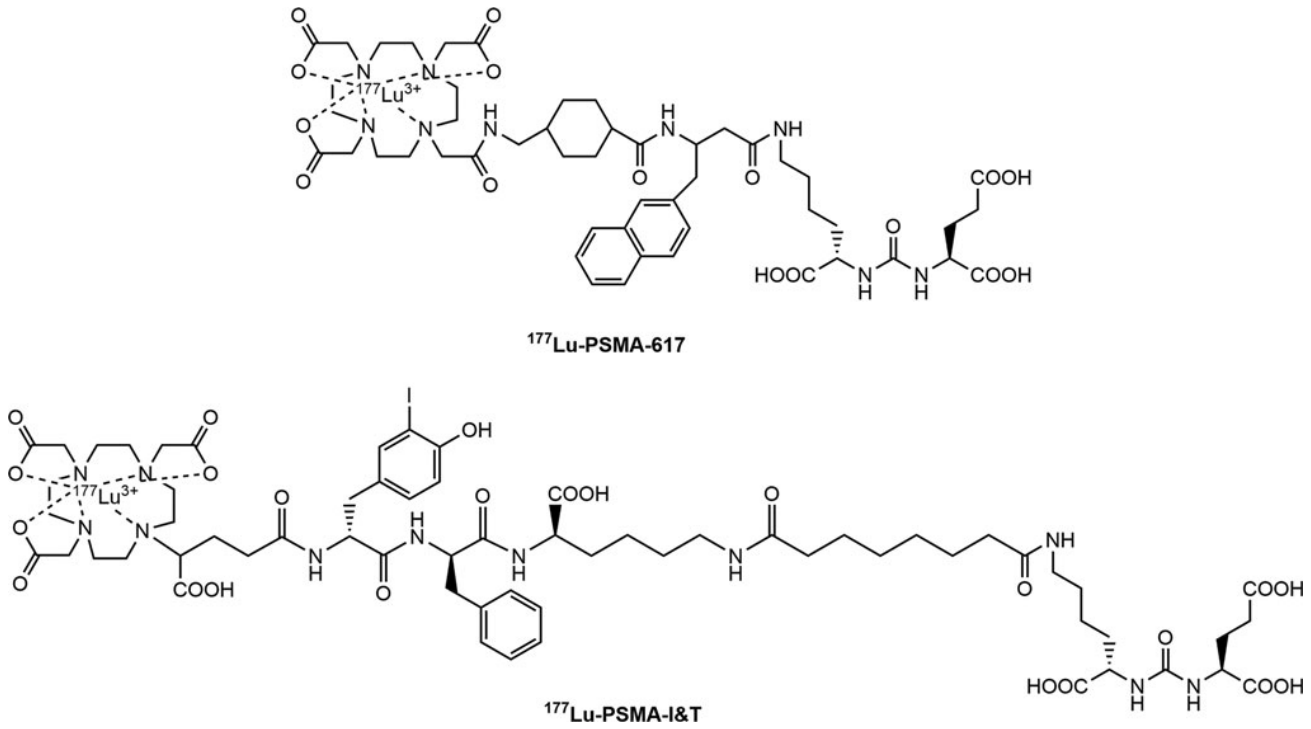

FIG. 6. Chemical structures of ^{177}Lu-PSMA-617 and ^{177}Lu-PSMA I&T.

Downloaded by University of Texas MD Anderson Cancer Center from www.liebertpub.com at 03/16/23. For personal use only.

Perspectives of Research and Development

Use cyclotron-produced ^{68}Ga for ^{68}Ga radiopharmaceuticals

The dramatic rise in PET imaging with ^{68}Ga-labeled tracers during the last decade has been a result of increased interest in applying ^{68}Ga radiopharmaceuticals for theranostic purposes. The theranostic concept is when a diagnostic scan is first performed using a ^{68}Ga-labeled ligand then the same ligand is labeled with a therapeutic radionuclide (e.g., ^{90}Y, ^{177}Lu, or ^{188}Re) for treatment.[89–91] Currently, ^{68}Ga is commonly provided through ^{68}Ge/^{68}Ga

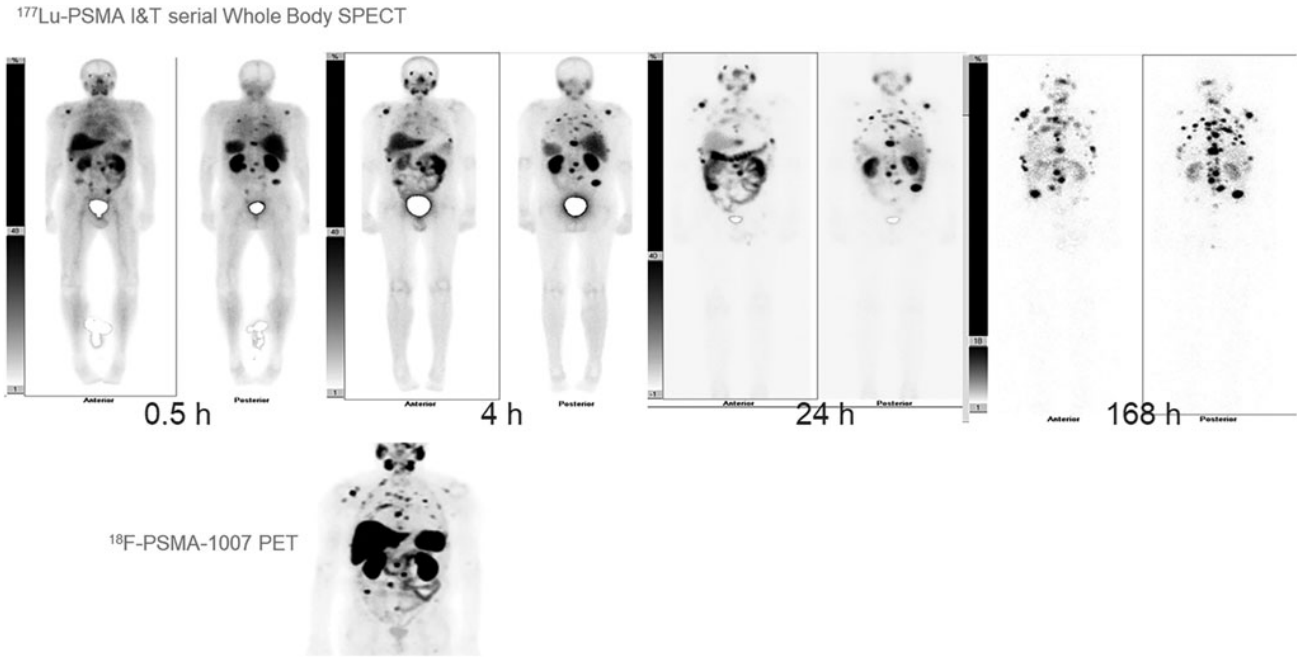

FIG. 7. ^{177}Lu-PSMA-I &T serial whole body at 0.5, 4, 24, and 168 h in a widespread advanced prostate cancer (bone and lymph node disease), AP/PA views. The diagnostic pretherapeutic ^{18}F-PSMA-1007 PET image is shown for comparison.

UH & EURATOM Exhibit 2042-009
Fusion v. Universität Heidelberg, et al.
IPR2023-00551

Downloaded by University of Texas MD Anderson Cancer Center from www.liebertpub.com at 03/16/23. For personal use only.

generators. Although high production volumes of the ^{68}Ge/^{68}Ga generators have recently been made to meet existing needs, there is a strong commercial appeal for cyclotron-produced ^{68}Ga to overcome limited availability of ^{68}Ga radiopharmaceuticals, particularly in densely populated regions. Consequently, the development of an alternative way to meet the increasing demand for ^{68}Ga is warranted.

Several attempts have been made to produce ^{68}Ga via ^{68}Zn(p,n)^{68}Ga reaction using a cyclotron. Jensen and Clark reported the first attempt to produce ^{68}Ga using a cyclotron with a liquid target filled with a $^{68}ZnCl_2$ solution.[92] Since then, other groups have tried to optimize ^{68}Ga production through liquid targetry.[93,94] Based on recent study performed by Alves et al., a liquid targetry containing 200 mg of ^{68}Zn resulted in 0.3 GBq/μA · h at the end of bombardment when the target was irradiated with 14.2 MeV protons.[93] Overall, producing ^{68}Ga using a liquid target is advantageous in minimizing radiation exposure during the target handling and processing. However, the available activity of ^{68}Ga from this technique is not significantly higher than activity obtained through a generator. In addition, the liquid target is with risk of excessive pressure during irradiation and requires more maintenances in the target and transfer lines that may limit its use for routine clinical productions.[94,95]

The possibility of producing ^{68}Ga with a solid target was first explored by Engle et al. using ^{nat}Zn as the target material.[96] Derived from cross-section measurements, the theoretical production yield can be up to 5.81 GBq/μA · h when an enriched ^{68}Zn solid target is irradiated by 15 MeV proton[97]; however, high zinc and HCl acid contents in the final ^{68}Ga solution are two potential challenges for cyclotron-produced ^{68}Ga. Although most ^{68}Zn can be removed using the AG50W cation resin alone,[93,94,96] additional processing is usually required to reconstitute ^{68}Ga solution with a low concentration of HCl for radiolabeling use. Considering the relatively short half-life of ^{68}Ga, a simple, fast, and cost-efficient processing procedure of ^{68}Ga post target irradiation is required.

In the Cyclotron Radiochemistry Facility at MD Anderson Cancer Center, the authors have developed a reliable and cost-efficient procedure for cyclotron produced ^{68}Ga, using solid target and chemical separation that are high in quality and yield.[98] In response to the need for a more efficient and economically viable alternative and to explore the potential applications of cyclotron-produced ^{68}Ga in routine radiopharmaceutical preparation, the authors have developed a simple and fully automated method of producing cGMP ^{68}Ga-PSMA-11 using cyclotron-produced ^{68}Ga and verified its biological equivalence. Preliminary data indicate the potential for large scale production of ^{68}Ga radiopharmaceuticals that can meet the increasing demand and facilitate regional distribution of these imaging agents.[99] Current development of ^{68}Zn pressed target is underway to reduce time for target preparation and further establish a more efficient way to produce ^{68}Ga on a routine daily basis.

Apply Al^{18}F as an alternative ^{18}F-labeling technique for PSMA-targeted molecules

Due to longer half-life of ^{18}F ($t_{1/2}$ = 109.8 min) allowing both imaging studies over a few hours and easier local distribution, radiolabeling PSMA molecules with ^{18}F represents an attractive alternative to its ^{68}Ga-based counterpart. In fact, recent clinical trials of both ^{18}F-DCFPyL and ^{18}F-PSMA-1007 have exhibited excellent sensitivity for the detection of biochemical recurrent prostate cancer as previously described. However, the precursors of both ^{18}F-DCFPyL and ^{18}F-PSMA-1007 have proprietary ownership (Progenics Pharmaceuticals and ABX, respectively) and have limited availability. Therefore, it would be advantageous to have other economically viable alternatives of ^{18}F-labeled PSMA tracers for PET imaging.

The labeling of biomolecules such as peptides through Al[^{18}F]-chelation is a new approach that was originally patented by Immunomedics, Inc.[100] and has recently received much attention. In this method, $^{18}F^-$ is first bound to Al^{3+} to form an aluminum fluoride moiety and then chelated by a suitable chelator. When the chelator is attached to a molecule of interest, radiolabeling the molecule with ^{18}F becomes possible.[101] As the hexadentate ligand *N*, *N*-bis(2-hydroxybenzyl) ethylenediamine-*N*,*N*-diacetic acid has shown a strong affinity toward Al[^{18}F]-based radiolabeling, due to its fast chelating kinetics at room temperature and favorable stability constant (log K = 24.8) with aluminum, labeling PSMA-11 with ^{18}F through Al[^{18}F] is reliably rapid, usually within 15 min at room temperature.[102,103] This success combines the proven pharmacophore with an ideal PET isotope for PSMA imaging.

According to preclinical evaluations performed by Lütje et al., Al[^{18}F]-PSMA-11 is unstable in water, but has a high internalization rate in PSMA-expressing tumors and lower renal accumulation compared to ^{68}Ga-PSMA-11.[104] A recent clinical study performed in 15 patients at Uruguayan Center of Molecular Imaging showed that a significantly higher SUV_{max} ratio for Al[^{18}F]-PSMA-11 compared to ^{68}Ga-PSMA-11 was observed (median value: 10.7 vs. 6.0).[105] The data suggest that Al[^{18}F]-PSMA-11 PET/CT is a promising imaging technique for the evaluation of patients with prostate cancer. To facilitate the clinical application of Al[^{18}F]-PSMA-11, the authors have recently developed the fully automated procedure as a simple single-step one-pot reaction in a modified TRACERlab FXN synthesis module (GE Healthcare, Chicago, IL). Al[^{18}F]PSMA-11 can be reliably produced at the range of 1.11–1.85 GBq (300–500 mCi; ≥95% radiochemical purity) in their current setting, with up to 60% radiochemical yield (nondecayed corrected) and the total synthetic time <30 min. In addition, the authors have successfully overcome the stability issue using 10 mM phosphate-buffered saline with 8% EtOH as the formulated solution, in which Al[^{18}F]PSMA-11 remains stable during the observation process at room temperature.

In addition to Al[^{18}F]PSMA-11, Al[^{18}F]PSMA-BCH has also been recently developed and showed excellent detectability of tumor lesions.[106] All of these indicate that Al[^{18}F] can be a convenient labeling strategy that has a great potential to accelerate the preparation of ^{18}F radiopharmaceuticals in PSMA-targeted imaging.

Develop J591 antibody fragments to optimize pharmacokinetics

As previously discussed, J591 has great targeting capability toward PSMA but suffers from slow tumor uptake *in vivo*. However, compared to PSMA inhibitor-based

UH & EURATOM Exhibit 2042-010
Fusion v. Universität Heidelberg, et al.
IPR2023-00551

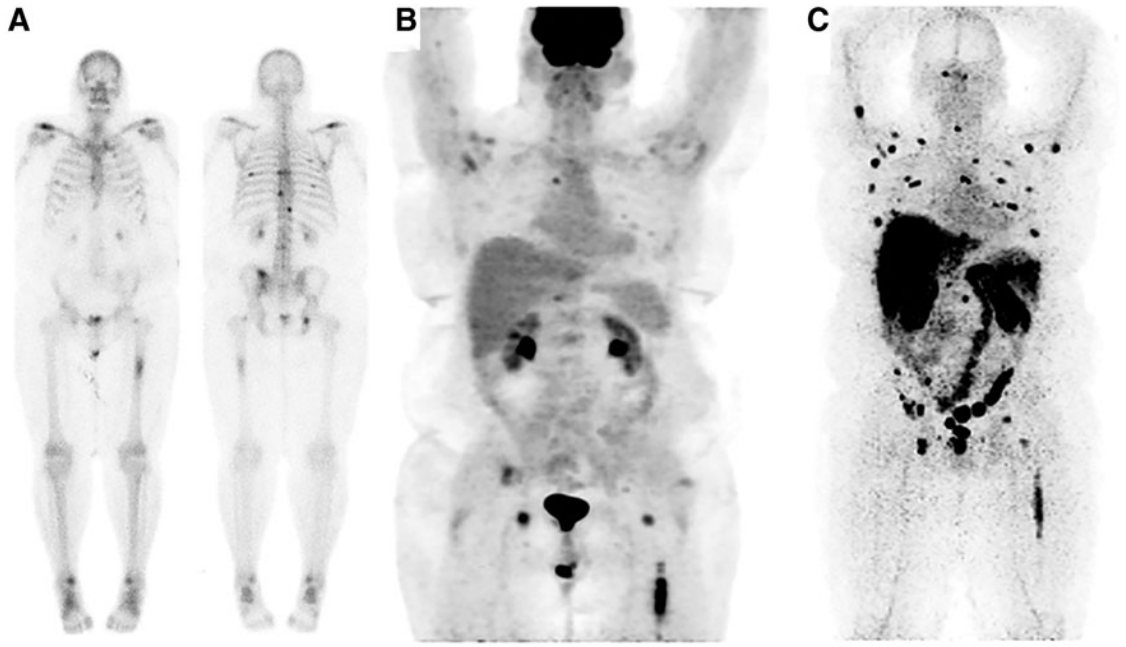

FIG. 8. Lesion targeting with ^{89}Zr-IAB2M in mPC patient. **(A)** ^{99m}Tc-MDP bone scan shows lesions in vertebrae and ribs. **(B)** ^{18}F-FDG PET scan shows uptake in left femur and faint uptake in vertebral lesions. **(C)** ^{89}Zr-IAB2M imaging shows more images than bone scanning or ^{18}F-FDG. Reprinted with permission from Journal of Nuclear Medicine, originally published by Pandit-Taskar et al.[108]

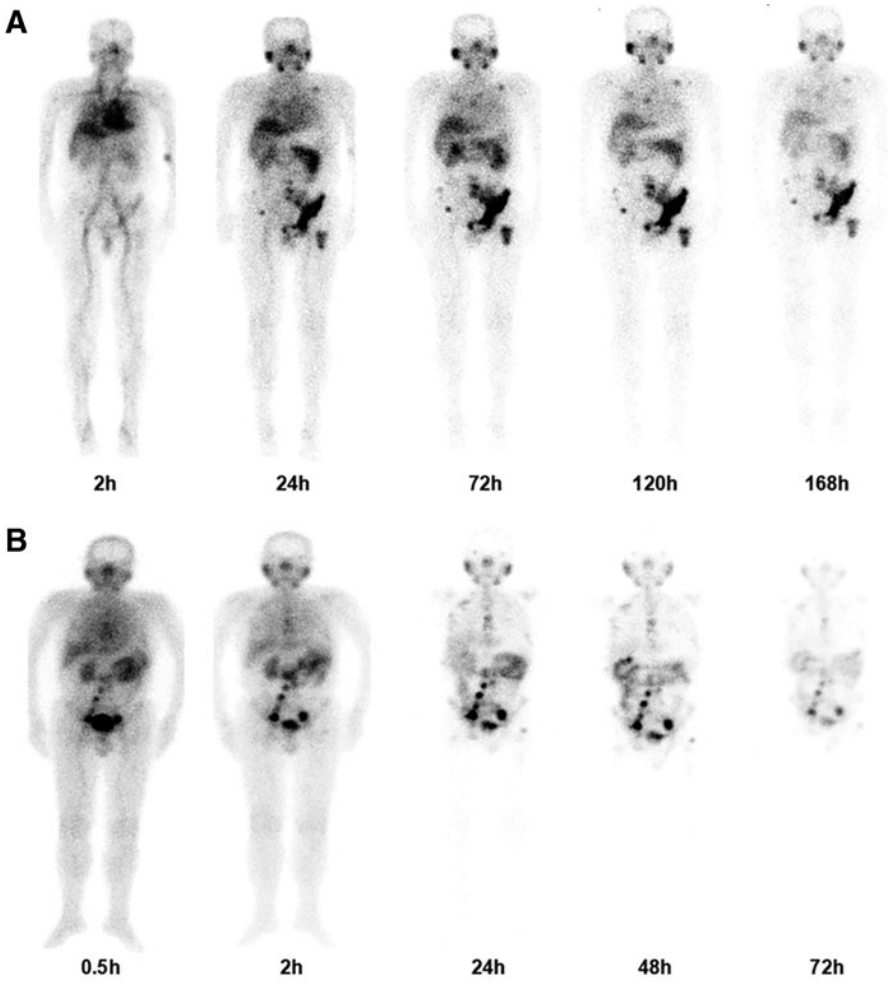

FIG. 9. **(A)** Representative whole-body anterior projection images of a 70-year-old male patient with mCRPC at different time points after intravenous administration of ^{177}Lu-EB-PSMA-617. **(B)** Representative whole-body anterior projection images of a 72-year-old male patient with mCRPC at different time points after intravenous administration of ^{177}Lu-PSMA-617. Reprinted with permission from European Journal of Nuclear Medicine and Molecular Imaging, originally published by Zang et al.[119]

Downloaded by University of Texas MD Anderson Cancer Center from www.liebertpub.com at 03/16/23. For personal use only.

UH & EURATOM Exhibit 2042-011
Fusion v. Universität Heidelberg, et al.
IPR2023-00551

Downloaded by University of Texas MD Anderson Cancer Center from www.liebertpub.com at 03/16/23. For personal use only.

radiopharmaceuticals, the accumulation of J591 in salivary gland is significantly lower for minimizing the occurrence of xerostomia. Therefore, studies have been focused on downsizing J591 to improve its pharmacokinetics.[107–111] One of the most promising studies using this concept is an anti-PSMA minibody, ^{89}Zr-Df-IAB2M, which has been recently evaluated in 15 patients and demonstrated favorable biodistribution and kinetics for targeting metastatic prostate cancer (Fig. 8).[108] Further investigations may reveal the potential of IAB2M in PSMA TAT when the molecule is labeled with alpha-emitters such as ^{212}Pb and ^{225}Ac.

Utilize albumin binding moieties to enhance overall tumor uptake

Plasma protein binding can be an effective strategy to improve the pharmacokinetic properties in decreasing clearance rate, as well as enhancing specific uptake of drugs.[112] As a result, several investigations have been focused on optimizing the biodistribution of low molecular weight PSMA ligands through the introduction of an albumin binding moiety.[113–116] A noteworthy process is conjugating Evans Blue, a strong albumin binding moiety, with a therapeutic PSMA-inhibitor, which has been currently investigated by several groups.[117–119] In a first proof-of-concept study, ^{177}Lu-PSMA-617 conjugated with Evans Blue (^{177}Lu-EB-PSMA-617) was evaluated in 9 patients with metastatic castration-resistant prostate cancer. The tumor uptake was about 2.15-fold higher than that in patients receiving ^{177}Lu-PSMA-617 (Fig. 9).[119] Although higher uptakes in kidneys and red bone marrow of ^{177}Lu-EB-PSMA-617 are also observed compared to ^{177}Lu-PSMA-617, the treatment was well tolerated in this pilot study at low doses. Further clinical studies with increasing therapeutic dose and frequency of ^{177}Lu-EB-PSMA-617 administration will be needed to fully investigate the benefit of utilizing albumin binding moieties in PSMA ligands.

Radiohybrid PSMA inhibitors as a new generation of theranostic agents

With the aim to efficiently label peptide-based radiopharmaceuticals such as PSMA inhibitors with either ^{18}F or radiometals, a new generation of radiopharmaceuticals named radhybrid PSMA (rhPSMA) ligands has recently been developed by Wurzer et al.[120] A unique feature of such rhPSMA ligands is that both fluorine and the metal are always present, but only one of them as radioactive isotope (e.g., [^{18}F,^{nat}Lu]rhPSMA or [^{19}F,^{177}Lu]rhPSMA). As chemically identical twins, rhPSMA could be used to bridge imaging and therapy. For example, information regarding dosimetry and/or therapeutic monitoring can be acquired from [^{18}F,^{nat}Lu]rhPSMA imaging, while [^{19}F,^{177}Lu]rhPSMA can be used for corresponding PSMA RLT. Recent report of ^{18}F-rhPSMA-7 demonstrates its strong potential in imaging patients with prostate cancer.[121] It has currently been licensed by Blue Earth Diagnostics for further clinical development.[122]

Conclusions

Over the last decade, the development of radiopharmaceuticals for PSMA-targeted imaging and therapy has become one of the most active and dynamic fields of research in nuclear medicine. According to Chang et al., 80.2% of prostate malignant cells overexpress PSMA, and the expression of PSMA correlates well with serum PSA concentration.[5] Therefore, there is little doubt that PSMA will remain an important focus of research in both academia and industrial companies. At this stage, there are several ongoing clinical trials of PSMA-targeted radiopharmaceuticals. Results of prospective phase III clinical trials will soon be available to reveal the diagnostic/therapeutic benefits on the predetermined endpoints of these agents.

Authors' Contributions

Each named author has substantially contributed to drafting this article. M.L.: Draft the outline and determine the subtopics of this article; lead the research of ^{68}Ga production and Al[^{18}F] radiolabeling in the facility. R.T.T.: Summarize the development of radiopharmaceuticals in PSMA-targeted imaging and therapy; provide their recent progress in ^{68}Ga production through a medical cyclotron and the synthesis of Al[^{18}F]PSMA-11. K.K.: Provide the detailed description and clinical data regarding ^{68}Ga-PSMA-11, ^{177}Lu-PSMA-617, and ^{177}Lu-PSMA I&T. D.B.L.: Assist data interpretation and article preparation. G.C.R.: Supervise the data collection and article preparation. The article has been read and approved for submission by all the named authors.

Disclosure Statement

Dr. Gregory C. Ravizzini is the recipient of research funding from Blue Earth Diagnostics and Advanced Accelerator Applications.

Funding Information

This work is supported by the CABI reinvestment fund through the University of Texas MD Anderson Cancer Center.

References

1. Siegel RL, Miller KD, Jemal A. Cancer statistics, 2019. CA Cancer J Clin 2019;69:7.
2. Han S, Woo S, Kim YJ, et al. Impact of ^{68}Ga-PSMA PET on the management of patients with prostate cancer: A systematic review and meta-analysis. Eur Urol 2018;74: 179.
3. Eifler JB, Feng Z, Lin BM, et al. An updated prostate cancer staging nomogram (Partin tables) based on cases from 2006 to 2011. BJU Int 2013;111:22.
4. Wibmer AG, Hricak H, Ulaner GA, et al. Trends in oncologic hybrid imaging. Eur J Hybrid Imaging 2018;2:1.
5. Chang SS. Overview of prostate-specific membrane antigen. Rev Urol 2004;6(Suppl 10):S13.
6. Davis MI, Bennett MJ, Thomas LM, et al. Crystal structure of prostate-specific membrane antigen, a tumor marker and peptidase. Proc Natl Acad Sci U S A 2005; 102:5981.
7. Troyer JK, Feng Q, Beckett ML, et al. Biochemical characterization and mapping of the 7E11-C5.3 epitope of the prostate-specific membrane antigen. Urol Oncol 1995; 1:29.
8. Gong MC, Chang SS, Sadelain M, et al. Prostate-specific membrane antigen (PSMA)-specific monoclonal antibodies in the treatment of prostate and other cancers. Cancer Metastasis Rev 1999;18:483.

UH & EURATOM Exhibit 2042-012
Fusion v. Universität Heidelberg, et al.
IPR2023-00551

Downloaded by University of Texas MD Anderson Cancer Center from www.liebertpub.com at 03/16/23. For personal use only.

9. Elgamal A-AA, Holmes EH, Su SL, et al. Prostate-specific membrane antigen (PSMA): Current benefits and future value. Semin Surg Oncol 2000;18:10.
10. Ghosh A, Heston WDW. Tumor target prostate specific membrane antigen (PSMA) and its regulation in prostate cancer. J Cell Biochem 2004;91:528.
11. Lenzo NP, Meyrick D, Turner JH. Review of gallium-68 PSMA PET/CT imaging in the management of prostate cancer. Diagnostics (Basel) 2018;8:pii:E16.
12. Sodee DB, Malguria N, Faulhaber P, et al. Multicenter ProstaScint imaging findings in 2154 patients with prostate cancer11A complete list of the ProstaScint Imaging Centers is provided in the Appendix. Urology 2000;56: 988.
13. Petronis JD, Regan F, Lin K. Indium-111 capromab pendetide (ProstaScint) Imaging to detect recurrent and metastatic prostate cancer. Clin Nucl Med 1998;23:672.
14. Haseman MK, Reed NL, Rosenthal SA. Monoclonal antibody imaging of occult prostate cancer in patients with elevated prostate-specific antigen. Positron emission tomography and biopsy correlation. Clin Nucl Med 1996; 21:704.
15. Polascik TJ, Manyak MJ, Haseman MK, et al. Comparison of clinical staging algorithms and 111indium-capromab pendetide immunoscintigraphy in the prediction of lymph node involvement in high risk prostate carcinoma patients. Cancer 1999;85:1586.
16. Apolo AB, Pandit-Taskar N, Morris MJ. Novel tracers and their development for the imaging of metastatic prostate cancer. J Nucl Med 2008;49:2031.
17. Smith-Jones PM, Vallabhajosula S, Navarro V, et al. Radiolabeled monoclonal antibodies specific to the extracellular domain of prostate-specific membrane antigen: Preclinical studies in nude mice bearing LNCaP human prostate tumor. J Nucl Med 2003;44:610.
18. Holland JP, Divilov V, Bander NH, et al. 89Zr-DFO-J591 for immunoPET of prostate-specific membrane antigen expression in vivo. J Nucl Med 2010;51:1293.
19. Pandit-Taskar N, Donoghue JA, Durack JC, et al. A phase I/II study for analytic validation of ^{89}Zr-J591 immunoPET as a molecular imaging agent for metastatic prostate cancer. Clin Cancer Res 2015;21:5277.
20. Fernández-García EM, Vera-Badillo FE, Perez-Valderrama B, et al. Immunotherapy in prostate cancer: Review of the current evidence. Clin Transl Oncol 2015; 17:339.
21. McDevitt MR, Barendswaard E, Ma D, et al. An α-particle emitting antibody ([^{213}Bi]J591) for radioimmunotherapy of prostate cancer. Cancer Res 2000;60:6095.
22. Vallabhajosula S, Goldsmith SJ, Kostakoglu L, et al. Radioimmunotherapy of prostate cancer using ^{90}Y- and ^{177}Lu-labeled J591 monoclonal antibodies: Effect of multiple treatments on myelotoxicity. Clin Cancer Res 2005;11:7195s.
23. Vallabhajosula S, Nikolopoulou A, Jhanwar YS, et al. Radioimmunotherapy of metastatic prostate cancer with ^{177}Lu-DOTAhuJ591 anti prostate specific membrane antigen specific monoclonal antibody. Curr Radiopharm 2016;9:44.
24. Rawlings ND, Barrett AJ. Structure of membrane glutamate carboxypeptidase. Biochim Biophys Acta 1997; 1339:247.
25. O'Keefe DS, Bacich DJ, Huang SS, et al. A perspective on the evolving story of PSMA biology, PSMA-based imaging, and endoradiotherapeutic strategies. J Nucl Med 2018;59:1007.
26. Jackson PF, Cole DC, Slusher BS, et al. Design, synthesis, and biological activity of a potent inhibitor of the neuropeptidase N-acetylated α-linked acidic dipeptidase. J Med Chem 1996;39:619.
27. Ding P, Helquist P, Miller MJ. Design, synthesis and pharmacological activity of novel enantiomerically pure phosphonic acid-based NAALADase inhibitors. Org Biomol Chem 2007;5:826.
28. Chakravarty R, Siamof CM, Dash A, et al. Targeted α-therapy of prostate cancer using radiolabeled PSMA inhibitors: A game changer in nuclear medicine. Ame J Nucl Med Mol Imaging 2018;8:247.
29. Majer P, Jackson PF, Delahanty G, et al. Synthesis and biological evaluation of thiol-based inhibitors of glutamate carboxypeptidase II: Discovery of an orally active GCP II inhibitor. J Med Chem 2003;46:1989.
30. Stoermer D, Liu Q, Hall MR, et al. Synthesis and biological evaluation of hydroxamate-Based inhibitors of glutamate carboxypeptidase II. Bioorg Med Chem Lett 2003;13:2097.
31. Blank BR, Alayoglu P, Engen W, et al. N-substituted glutamyl sulfonamides as inhibitors of glutamate carboxypeptidase II (GCP2). Chem Biol Drug Des 2011;77: 241.
32. Majer P, Hin B, Stoermer D, et al. Structural optimization of thiol-based inhibitors of glutamate carboxypeptidase II by modification of the P1'side chain. J Med Chem 2006; 49:2876.
33. Pomper MG, Musachio JL, Zhang J, et al. 11C-MCG: Synthesis, uptake selectivity, and primate PET of a probe for glutamate carboxypeptidase II (NAALADase). Mol Imaging 2002;1:96.
34. Foss CA, Mease RC, Fan H, et al. Radiolabeled small-molecule ligands for prostate-specific membrane antigen: In vivo imaging in experimental models of prostate cancer. Clin Cancer Res 2005;11:4022.
35. Pillai MRA, Nanabala R, Joy A, et al. Radiolabeled enzyme inhibitors and binding agents targeting PSMA: Effective theranostic tools for imaging and therapy of prostate cancer. Nucl Med Biol 2016;43:692.
36. Barrett JA, Coleman RE, Goldsmith SJ, et al. First-in-man evaluation of 2 high-affinity PSMA-avid small molecules for imaging prostate cancer. J Nucl Med 2013;54:380.
37. Afshar-Oromieh A, Haberkorn U, Zechmann C, et al. Repeated PSMA-targeting radioligand therapy of metastatic prostate cancer with ^{131}I-MIP-1095. Eur J Nucl Med Mol Imaging 2017;44:950.
38. Banerjee SR, Pullambhatla M, Shallal H, et al. A modular strategy to prepare multivalent inhibitors of prostate-specific membrane antigen (PSMA). Oncotarget 2011;2:1244.
39. Ray Banerjee S, Pullambhatla M, Foss CA, et al. Effect of chelators on the pharmacokinetics of ^{99m}Tc-labeled imaging agents for the prostate-specific membrane antigen (PSMA). J Med Chem 2013;56:6108.
40. Lu G, Maresca KP, Hillier SM, et al. Synthesis and SAR of ^{99m}Tc/Re-labeled small molecule prostate specific membrane antigen inhibitors with novel polar chelates. Bioorg Med Chem Lett 2013;23:1557.
41. Santos-Cuevas C, Davanzo J, Ferro-Flores G, et al. ^{99m}Tc-labeled PSMA inhibitor: Biokinetics and radiation dosimetry in healthy subjects and imaging of prostate cancer tumors in patients. Nucl Med Biol 2017;52:1.

UH & EURATOM Exhibit 2042-013
Fusion v. Universität Heidelberg, et al.
IPR2023-00551

Downloaded by University of Texas MD Anderson Cancer Center from www.liebertpub.com at 03/16/23. For personal use only.

42. Schmidkonz C, Cordes M, Beck M, et al. SPECT/CT with the PSMA ligand ^{99m}Tc-MIP-1404 for whole-body primary staging of patients with prostate cancer. Clin Nucl Med 2018;43:225.
43. Vallabhajosula S, Nikolopoulou A, Babich JW, et al. ^{99m}Tc-labeled small-molecule inhibitors of prostate-specific membrane antigen: Pharmacokinetics and biodistribution studies in healthy subjects and patients with metastatic prostate cancer. J Nucl Med 2014;55:1791.
44. Schmidkonz C, Cordes M, Beck M, et al. Assessment of treatment response by ^{99m}Tc-MIP-1404 SPECT/CT: A pilot study in patients with metastatic prostate cancer. Clin Nucl Med 2018;43:e250.
45. Notni J, Wester HJ. Re-thinking the role of radiometal isotopes: Towards a future concept for theranostic radiopharmaceuticals. J Labelled Comp Radiopharm 2017;61: 141.
46. Hofmann M, Maecke H, Borner R, et al. Biokinetics and imaging with the somatostatin receptor PET radioligand ^{68}Ga-DOTATOC: Preliminary data. Eur J Nucl Med 2001;28:1751.
47. Afshar-Oromieh A, Haberkorn U, Eder M, et al. [^{68}Ga]Gallium-labelled PSMA ligand as superior PET tracer for the diagnosis of prostate cancer: Comparison with ^{18}F-FECH. Eur J Nucl Med Mol Imaging 2012;39:1085.
48. Caroli P, Sandler I, Matteucci F, et al. ^{68}Ga-PSMA PET/CT in patients with recurrent prostate cancer after radical treatment: Prospective results in 314 patients. Eur J Nucl Med Mol Imaging 2018;45:2035.
49. Castellucci P, Ceci F, Graziani T, et al. Early biochemical relapse after radical prostatectomy: Which prostate cancer patients may benefit from a restaging ^{11}C-Choline PET/CT scan before salvage radiation therapy? J Nucl Med 2014;55:1424.
50. Perera M, Papa N, Christidis D, et al. Sensitivity, specificity, and predictors of positive ^{68}Ga-prostate-specific membrane antigen positron emission tomography in advanced prostate cancer: A systematic review and meta-analysis. Eur Urol 2016;70:926.
51. Eissa A, El Sherbiny A, Coelho RF, et al. The role of ^{68}Ga-PSMA PET/CT scan in biochemical recurrence after primary treatment for prostate cancer: A systematic review of literature. Minerva Urol Nefrol 2018;70:462.
52. Corfield J, Perera M, Bolton D, et al. ^{68}Ga-prostate specific membrane antigen (PSMA) positron emission tomography (PET) for primary staging of high-risk prostate cancer: A systematic review. World J Urol 2018;36:519.
53. von Eyben FE, Picchio M, von Eyben R, et al. ^{68}Ga-labeled prostate-specific membrane antigen ligand positron emission tomography/computed tomography for prostate cancer: A systematic review and meta-analysis. Eur Urol Focus 2016;4:686.
54. Calais J, Fendler WP, Herrmann K, et al. Comparison of ^{68}Ga-PSMA-11 and ^{18}F-fluciclovine PET/CT in a case series of 10 patients with prostate cancer recurrence. J Nucl Med 2018;59:789.
55. Lutje S, Heskamp S, Cornelissen AS, et al. PSMA ligands for radionuclide imaging and therapy of prostate cancer: Clinical status. Theranostics 2015;5:1388.
56. Al-Momani E, Israel I, Samnick S. Validation of a [Al^{18}F]PSMA-11 preparation for clinical applications. Appl Radiat Isot 2017;130:102.
57. Afshar-Oromieh A, Hetzheim H, Kratochwil C, et al. The theranostic PSMA ligand PSMA-617 in the diagnosis of prostate cancer by PET/CT: Biodistribution in humans, radiation dosimetry, and first evaluation of tumor lesions. J Nucl Med 2015;56:1697.
58. Derlin T, Schmuck S, Juhl C, et al. Imaging characteristics and first experience of [^{68}Ga]THP-PSMA, a novel probe for rapid kit-based Ga-68 labeling and PET imaging: Comparative analysis with [^{68}Ga]PSMA I&T. Mol Imaging Biol 2018;20:650.
59. Derlin T, Schmuck S, Juhl C, et al. PSA-stratified detection rates for [^{68}Ga]THP-PSMA, a novel probe for rapid kit-based ^{68}Ga-labeling and PET imaging, in patients with biochemical recurrence after primary therapy for prostate cancer. Eur J Nucl Med Mol Imaging 2018;45:913.
60. Benesova M, Schafer M, Bauder-Wust U, et al. Preclinical evaluation of a tailor-made DOTA-conjugated PSMA inhibitor with optimized linker moiety for imaging and endoradiotherapy of prostate cancer. J Nucl Med 2015;56: 914.
61. Prasad V, Steffen IG, Diederichs G, et al. Biodistribution of [^{68}Ga]PSMA-HBED-CC in patients with prostate cancer: Characterization of uptake in normal organs and tumour lesions. Mol Imaging Biol 2016;18:428.
62. Kabasakal L, Demirci E, Ocak M, et al. Evaluation of PSMA PET/CT imaging using a ^{68}Ga-HBED-CC ligand in patients with prostate cancer and the value of early pelvic imaging. Nucl Med Commun 2015;36:582.
63. Perveen G, Arora G, Damle NA, et al. Role of early dynamic positron emission tomography/computed tomography with ^{68}Ga-prostate-specific membrane antigen-HBED-CC in patients with adenocarcinoma prostate: Initial results. Indian J Nucl Med 2018;33:112.
64. Mease RC, Dusich CL, Foss CA, et al. *N*-[*N*-[(S)-1,3-dicarboxypropyl]carbamoyl]-4-[18F]fluorobenzyl-L-cysteine, [^{18}F]DCFBC: A new imaging probe for prostate cancer. Clin Cancer Res 2008;14:3036.
65. Cho SY, Gage KL, Mease RC, et al. Biodistribution, tumor detection, and radiation dosimetry of ^{18}F-DCFBC, a low-molecular-weight inhibitor of prostate-specific membrane antigen, in patients with metastatic prostate cancer. J Nucl Med 2012;53:1883.
66. Rowe SP, Macura KJ, Ciarallo A, et al. Comparison of prostate-specific membrane antigen-based ^{18}F-DCFBC PET/CT to conventional imaging modalities for detection of hormone-naïve and castration-resistant metastatic prostate cancer. J Nucl Med 2016;57:46.
67. Turkbey B, Mena E, Lindenberg L, et al. ^{18}F-DCFBC prostate-specific membrane antigen-targeted PET/CT imaging in localized prostate cancer: Correlation with multiparametric MRI and histopathology. Clin Nucl Med 2017;42:735.
68. Chen Y, Pullambhatla M, Foss CA, et al. 2-(3-{1-Carboxy-5-[(6-[^{18}F]fluoro-pyridine-3-carbonyl)-amino]-pentyl}-ureido)-pentanedioic acid, [^{18}F]DCFPyL, a PSMA-based PET imaging agent for prostate cancer. Clin Cancer Res 2011;17:7645.
69. Szabo Z, Mena E, Rowe SP, et al. Initial evaluation of [^{18}F]DCFPyL for prostate-specific membrane antigen (PSMA)-targeted PET imaging of prostate cancer. Mol Imaging Biol 2015;17:565.
70. Rowe SP, Mana-ay M, Javadi MS, et al. PSMA-based detection of prostate cancer bone lesions with ^{18}F-DCFPyL PET/CT: A sensitive alternative to ^{99m}Tc-MDP bone scan and Na^{18}F PET/CT? Clin Genitourin Cancer 2016;14:e115.

UH & EURATOM Exhibit 2042-014
Fusion v. Universität Heidelberg, et al.
IPR2023-00551

Downloaded by University of Texas MD Anderson Cancer Center from www.liebertpub.com at 03/16/23. For personal use only.

71. Wondergem M, Jansen BHE, van der Zant FM, et al. Early lesion detection with ^{18}F-DCFPyL PET/CT in 248 patients with biochemically recurrent prostate cancer. Eur J Nucl Med Mol Imaging 2019;46:1911.
72. Giesel FL, Hadaschik B, Cardinale J, et al. F-18 labelled PSMA-1007: Biodistribution, radiation dosimetry and histopathological validation of tumor lesions in prostate cancer patients. Eur J Nucl Med Mol Imaging 2017;44: 678.
73. Treglia G, Annunziata S, Pizzuto DA, et al. Detection rate of ^{18}F-labeled PSMA PET/CT in biochemical recurrent prostate cancer: A systematic review and a meta-analysis. Cancers 2019;11:710.
74. Rahbar K, Weckesser M, Ahmadzadehfar H, et al. Advantage of ^{18}F-PSMA-1007 over ^{68}Ga-PSMA-11 PET imaging for differentiation of local recurrence vs. urinary tracer excretion. Eur J Nucl Med Mol Imaging 2018;45: 1076.
75. Giesel FL, Will L, Lawal I, et al. Intraindividual comparison of ^{18}F-PSMA-1007 and ^{18}F-DCFPyL PET/CT in the prospective evaluation of patients with newly diagnosed prostate carcinoma: A pilot study. J Nucl Med 2018;59:1076.
76. Strosberg J, El-Haddad G, Wolin E, et al. Phase 3 trial of ^{177}Lu-Dotatate for midgut neuroendocrine tumors. N Engl J Med 2017;376:125.
77. Rahbar K, Ahmadzadehfar H, Kratochwil C, et al. Safety and efficacy of ^{177}Lu-PSMA-617 radioligand therapy in patients with mCRPC: A multicenter study. J Clin Oncol 2017;35(6_Suppl):155.
78. Roll W, Bode A, Weckesser M, et al. Excellent eesponse to ^{177}Lu-PSMA-617 radioligand therapy in a patient with advanced metastatic castration resistant prostate cancer evaluated by ^{68}Ga-PSMA PET/CT. Clin Nucl Med 2017;42:152.
79. van Kalmthout L, Braat A, Lam M, et al. First experience with ^{177}Lu-PSMA-617 therapy for advanced prostate cancer in the netherlands. Clin Nucl Med 2019; 44:446.
80. Zhang J, Kulkarni HR, Singh A, et al. ^{177}Lu-PSMA-617 radioligand therapy in metastatic castration-resistant prostate cancer patients with a single functioning kidney. J Nucl Med 2019;60:1579.
81. Yadav MP, Ballal S, Sahoo RK, et al. Radioligand therapy with ^{177}Lu-PSMA for metastatic castration-resistant prostate cancer: A systematic review and meta-analysis. Am J Roentgenol 2019;213:275.
82. Yadav MP, Ballal S, Tripathi M, et al. ^{177}Lu-DKFZ-PSMA-617 therapy in metastatic castration resistant prostate cancer: Safety, efficacy, and quality of life assessment. Eur J Nucl Med Mol Imaging 2017;44:81.
83. Yadav MP, Ballal S, Bal C, et al. Efficacy and safety of ^{177}Lu-PSMA-617 radioligand therapy in metastatic castration-resistant prostate cancer patients. Clin Nucl Med 2020;45:19.
84. Kulkarni HR, Singh A, Schuchardt C, et al. PSMA-based radioligand therapy for metastatic castration-resistant prostate cancer: The bad berka experience since 2013. J Nucl Med 2016;57(Suppl 3):97S.
85. Kairemo K, Joensuu T. Lu-177-PSMA treatment for metastatic prostate cancer: Case examples of major responses. Clin Transl Imaging 2018;6:223.
86. von Eyben FE, Roviello G, Kiljunen T, et al. Third-line treatment and ^{177}Lu-PSMA radioligand therapy of metastatic castration-resistant prostate cancer: A systematic review. Eur J Nucl Med Mol imaging 2018;45:496.
87. Kratochwil C, Bruchertseifer F, Giesel FL, et al. ^{225}Ac-PSMA-617 for PSMA-targeted alpha-radiation therapy of metastatic castration-resistant prostate cancer. J Nucl Med 2016;57:1941.
88. Sathekge M, Bruchertseifer F, Knoesen O, et al. ^{225}Ac-PSMA-617 in chemotherapy-naive patients with advanced prostate cancer: A pilot study. Eur J Nucl Med Mol imaging 2019;46:129.
89. Verger E, Drion P, Meffre G, et al. ^{68}Ga and ^{188}Re starch-based microparticles as theranostic tool for the hepatocellular carcinoma: Radiolabeling and preliminary in vivo rat studies. PLoS One 2016;11:e0164626.
90. Weineisen M, Schottelius M, Simecek J, et al. ^{68}Ga- and ^{177}Lu-labeled PSMA I&T: Optimization of a PSMA-targeted theranostic concept and first proof-of-concept human studies. J Nucl Med 2015;56:1169.
91. Koukouraki S, Strauss LG, Georgoulias V, et al. Comparison of the pharmacokinetics of ^{68}Ga-DOTATOC and [^{18}F]FDG in patients with metastatic neuroendocrine tumours scheduled for 90Y-DOTATOC therapy. Eur J Nucl Med Mol Imaging 2006;33:1115.
92. Jensen M, Clark J. Direct production of Ga-68 from proton bombardment of concentrated aqueous solutions of [Zn-68] zinc chloride. The 13th International Workshop on Targetry and Target Chemistry Proceedings, Roskilde, Denmark, 2011:288.
93. Alves F, Alves VHP, Do Carmo SJC, et al. Production of copper-64 and gallium-68 with a medical cyclotron using liquid targets. Modern Phys Lett A 2017;32:1740013.
94. Pandey MK, Byrne JF, Jiang H, et al. Cyclotron production of ^{68}Ga via the ^{68}Zn(p,n)^{68}Ga reaction in aqueous solution. Am J Nucl Med Mol Imaging 2014;4: 303.
95. Alves F, Alves VH, Neves ACB, et al. Cyclotron production of Ga-68 for human use from liquid targets: From theory to practice. AIP Conf Proc 2017;1845:020001.
96. Engle JW, Lopez-Rodriguez V, Gaspar-Carcamo RE, et al. Very high specific activity ^{68}Ga from zinc targets for PET. Appl Radiat Isot 2012;70:1792.
97. Szelecsényi F, Kovács Z, Nagatsu K, et al. Investigation of direct production of ^{68}Ga with low energy multiparticle accelerator. Radiochim Acta Int 2012;100:5.
98. Lin M, Waligorski GJ, Lepera CG. Production of curie quantities of ^{68}Ga with a medical cyclotron via the ^{68}Zn(p,n)^{68}Ga reaction. Appl Radiat Isot 2018;133:1.
99. Lin M, Paolillo V, Ta RT, et al. Fully automated preparation of 68Ga-PSMA-11 at curie level quantity using cyclotron-produced ^{68}Ga for clinical applications. Appl Radiat Isot 2019;155:108936.
100. Mcbride WJ, Christopher SAD, Goldenberg DM, et al. Methods and compositions for improved F-18 labeling of proteins, peptides and other molecules. Patent No. EP2117604A4
101. Price EW, Orvig C. Matching chelators to radiometals for radiopharmaceuticals. Chem Soc Rev 2014;43:260.
102. Malik N, Baur B, Winter G, et al. Radiofluorination of PSMA-HBED via Al^{18}F^{2+} chelation and biological evaluations in vitro. Mol Imaging Biol 2015;17:777.
103. Boschi S, Lee JT, Beykan S, et al. Synthesis and preclinical evaluation of an Al^{18}F radiofluorinated GLU-UREA-LYS(AHX)-HBED-CC PSMA ligand. Eur J Nucl Med Mol Imaging 2016;43:2122.

UH & EURATOM Exhibit 2042-015
Fusion v. Universität Heidelberg, et al.
IPR2023-00551

104. Lütje S, Franssen GM, Herrmann K, et al. In vitro and in vivo characterization of a ^{18}F-AlF-labeled PSMA ligand for imaging of PSMA-expressing xenografts. J Nucl Med 2019;60:1017.
105. Alonso O, dos Santos G, Giglio J, et al. PET/CT evaluation of prostate cancer patients with Al^{18}F-PSMA-HBED-CC: A head-to-head comparison with ^{68}Ga-PSMA-HBED-CC. J Nucl Med 2018;59(Suppl 1):1499.
106. Liu T, Liu C, Xu X, et al. Preclinical evaluation and pilot clinical study of Al^{18}F-PSMA-BCH for prostate cancer PET imaging. J Nucl Med 2019;60:1284.
107. Morris MJ, Solomon SB, Durack JC, et al. Pathologic correlation of ^{89}Zr-Df-IAB2M antiprostate-specific membrane antigen (PSMA) minibody in patients with metastatic prostate cancer. J Clin Oncol 2015;33(7_Suppl):220.
108. Pandit-Taskar N, O'Donoghue JA, Ruan S, et al. First-in-human imaging with ^{89}Zr-Df-IAB2M anti-PSMA minibody in patients with metastatic prostate cancer: Pharmacokinetics, biodistribution, dosimetry, and lesion uptake. J Nucl Med 2016;57:1858.
109. Frigerio B, Franssen G, Luison E, et al. Full preclinical validation of the ^{123}I-labeled anti-PSMA antibody fragment ScFvD2B for prostate cancer imaging. Oncotarget 2017;8:10919.
110. Chatalic KL, Veldhoven-Zweistra J, Bolkestein M, et al. A novel ^{111}In-labeled anti-prostate-specific membrane antigen nanobody for targeted SPECT/CT imaging of prostate cancer. J Nucl Med 2015;56:1094.
111. Dekempeneer Y, Keyaerts M, Krasniqi A, et al. Targeted alpha therapy using short-lived alpha-particles and the promise of nanobodies as targeting vehicle. Expert Opin Biol Ther 2016;16:1035.
112. Dennis MS, Zhang M, Meng YG, et al. Albumin binding as a general strategy for improving the pharmacokinetics of proteins. J Biol Chem 2002;277:35035.
113. Kuo H-T, Merkens H, Zhang Z, et al. Enhancing treatment efficacy of ^{177}Lu-PSMA-617 with the conjugation of an albumin-binding motif: Preclinical dosimetry and endoradiotherapy studies. Mol Pharm 2018;15:5183.
114. Umbricht CA, Benešová M, Hasler R, et al. Design and preclinical evaluation of an albumin-binding PSMA ligand for ^{64}Cu-based PET imaging. Mol Pharm 2018;15:5556.
115. Benešová M, Umbricht CA, Schibli R, et al. Albumin-binding PSMA ligands: Optimization of the tissue distribution profile. Mol Pharm 2018;15:934.
116. Kelly JM, Amor-Coarasa A, Ponnala S, et al. Albumin-binding PSMA ligands: Implications for expanding the therapeutic window. J Nucl Med 2019;60:656.
117. Wang Z, Jacobson O, Tian R, et al. Radioligand therapy of prostate cancer with a long-lasting prostate-specific membrane antigen targeting agent ^{90}Y-DOTA-EB-MCG. Bioconjug Chem 2018;29:2309.
118. Wang Z, Tian R, Niu G, et al. Single low-dose injection of evans blue modified PSMA-617 radioligand therapy eliminates prostate-specific membrane antigen positive tumors. Bioconjug Chem 2018;29:3213.
119. Zang J, Fan X, Wang H, et al. First-in-human study of ^{177}Lu-EB-PSMA-617 in patients with metastatic castration-resistant prostate cancer. Eur J Nucl Med Mol Imaging 2019;46:148.
120. Wurzer A, Di Carlo D, Schmidt A, et al. PSMA-targeted^{18}F-labeled radiohybrid inhibitors: Concept, preclinical evaluation and first proof of concept study in men. J Nucl Med 2019;60(Suppl 1):344.
121. Oh SW, Wurzer A, Teoh E, et al. Quantitative and qualitative analysis of biodistribution and PET image quality of novel radiohybrid PSMA ligand, ^{18}F- rhPSMA-7, in patients with prostate cancer. J Nucl Med 2019;60(Suppl 1):1557.
122. Blue Earth Diagnostics Announces Results from Initial Clinical Experience of ^{18}F-rhPSMA-7 PET Imaging in High-risk Primary and Biochemical Recurrent Prostate Cancer by Technical University of Munich. May 7. Online document at http://blueearthdiagnostics.com/blue-earth-diagnostics-announces-results-from-initial-clinical-experience-of-18f-rhpsma-7-pet-imaging-in-high-risk-primary-and-biochemical-recurrent-prostate-cancer-by-technical-university-of-munich/ Accessed on March 03, 2020.

Downloaded by University of Texas MD Anderson Cancer Center from www.liebertpub.com at 03/16/23. For personal use only.

View publication stats

UH & EURATOM Exhibit 2042-016
Fusion v. Universität Heidelberg, et al.
IPR2023-00551